A Novel Electro-Thermal Model for Carbon Nanotube Interconnects

Walid Soliman, Tarek M. Abdolkader, Mohammed M. El-Banna and Salah H. Gamal.

Engineering Physics and Mathematics Department, Faculty of Engineering, Ain Shams University, Cairo, Egypt.
walidsol@yahoo.com

Abstract: The electro-thermal effects have an important role in the study of metallic Single-Wall Carbon Nanotubes (SWCNTs) for interconnect applications. Experimental data and careful modeling reveal that self-heating is considerably significant in short nanotubes ($1 < \boldsymbol{L} < 15\boldsymbol{\mu}$m) under high-bias. The low-bias resistance of micron scale SWCNTs is also found to be affected by optical phonon absorption (a scattering mechanism previously neglected) above 250 ***K***. In this work, we explore the effect of the thermo-electric current ($\boldsymbol{I_{hc}}$) caused by the temperature difference along the SWCNTs interconnects (thermo-electric properties). The thermo-electric current effect is studied at low and high lengths of SWCNTs and at different biases.

[Walid Soliman, Tarek M. Abdolkader, Mohammed M. El-Banna and Salah H. Gamal. **A Novel Electro Thermal Model for Carbon Nanotube Interconnects.** *J Am Sci* 2013;9(4):511-518]. (ISSN: 1545-1003). http://www.jofamericanscience.org. 55

Key Words: Electro-thermal Effects / Metallic Single-Wall Carbon Nanotubes / Thermo-electric Current Effect

Introduction:

Classic interconnect materials like Cu have limited current density of about 10^6 A/cm^2 and thermal conductivity of 401 Wm^{-1}K^{-1} at room temperature. CNTs can carry three orders of magnitude larger current densities than Cu (10^9A/cm^2) without showing signs of electromigration failure and have thermal conductivity 600–7000Wm^{-1}K^{-1} [1].

CNTs may behave as metallic or semiconducting as a result of their chirality. Metallic CNTs are suitable for interconnect applications while semiconducting CNTs are used for the implementation of nanoscale field effect transistors [2].

CNTs offer several advantages compared to Cu/low-κ interconnects due to four reasons. First, it has higher conductivity and this is because the phase space for electron scattering in CNTs is limited, and also because of their one-dimensional nature. The conductivity of densely-packed CNTs is higher than scaled Cu interconnects for large lengths. Conductivity of short CNT bundles, however, is limited by their quantum resistance. Metallic SWCNTs have two conduction channels, and their quantum resistance is 6.5 kΩ [3].

Second, more importantly, an isolated CNT can carry current densities in excess of 10^{10} A/cm^2 without any signs of damage even at an elevated temperature of 250 ˚C, thereby eliminating electromigration reliability concerns that plague nanoscale Cu interconnects [4].

Third, SWCNTs are stiff and strong, exhibiting Young's moduli in the range of 1–2 TPa, as inferred from properties of bundles and multi-walled tubes [5].

Finally, the thermal conductivity of nanotubes exceed that of copper by a factor of 15 and that of diamond by a factor of 2 and is, therefore, ideal for dissipating heat from sensitive active devices [6].

In this work we have proposed a thermally self-consistent resistance model suitable for circuit analysis and compared this model with previous models. It was found that due to optical phonon (OP) absorption above 250 K the low-bias resistance of SWCNTs with lengths relevant to interconnect applications (micro scale) increases with temperature. Moreover shorter SWCNT interconnects ($1 < \boldsymbol{L} < 15$ $\boldsymbol{\mu m}$) suffer relatively more from self-heating than longer tubes for the same total power dissipated. Our results have significant implications for the viability of SWCNT-based interconnects, and the proposed model covers a wide range of voltages and temperatures of practical relevance.

In section II, the electrical transport of SWCNTs interconnects is presented. In section III, we will illustrate thermal transport analysis, and then we will describe the novel electro-thermal transport model. Finally, results are presented and discussed in section IV.

Electrical Transport

Fig. 1 shows the SWCNT layout used for the analysis. It consists of two resistances $R_{contact}$ and R_{tube} and the distance ***d*** is the diameter of SWCNT. The thermal conductance from nanotube- and contacts-to-substrate is dominated by their interface, with $\boldsymbol{g} \approx 0.1$-0.2 WK^{-1}m^{-1} in this work. The temperature dependence of the resistance is obtained through the temperature dependence of the electron scattering Mean Free Paths (MFPs) with acoustic (AC) and optical (OP) phonons [7].

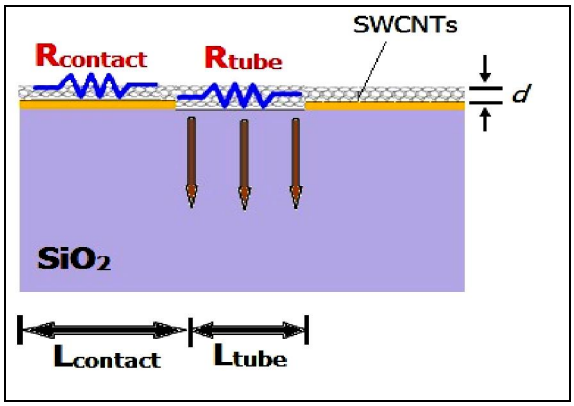

Fig. 1: Schematic of two-terminal SWCNTs device.

The total resistance is written as [8]

$$R(V,T) = R_c + \frac{h}{4q^2}\left[\frac{L+\lambda_{eff}(V,T)}{\lambda_{eff}(V,T)}\right] \quad (1)$$

where R_C is the electrical contact resistance, h is the Planck's constant, q is the electric charge and λ_{eff} is the net effective electron MFP. The total electron scattering Mean Free Paths (MFPs) is

$$\lambda_{eff} = \left(\lambda_{AC}^{-1} + \lambda_{OP,ems}^{-1} + \lambda_{OP,abs}^{-1}\right)^{-1} \quad (2)$$

which includes acoustic (AC) phonons, and electron scattering both by OP emission and absorption.
The AC scattering and OP absorption lengths can be written respectively as [7]:

$$\lambda_{AC} = \lambda_{AC,300}(300/T) \quad (3)$$

where $\lambda_{AC,300} \approx 1600$ nm is the AC scattering length at 300 K.

$$\lambda_{OP,abs}(T) = \lambda_{OP,300}\frac{N_{OP}(300)+1}{N_{OP}(T)} \quad (4)$$

where $\lambda_{OP,300} \approx 15$ nm is the spontaneous OP emission length at 300 K. The OP occupation number is given by $N_{OP} = 1/[\exp(\hbar\omega_{OP}/k_BT) - 1]$.

We note that OP emission can occur both after electrons gain sufficient energy from the electric field, and after an OP absorption event:

$$\lambda_{OP,ems} = \left(1/\lambda_{OP,ems}^{fld} + 1/\lambda_{OP,ems}^{abs}\right)^{-1} \quad (5)$$

The former MFP can be written as

$$\lambda_{OP,ems}^{fld}(T) = \frac{\hbar\omega_{OP}}{qV}L + \frac{N_{OP}(300)+1}{N_{OP}(T)+1}\lambda_{OP,300} \quad (6)$$

where the first term estimates the distance electrons must travel in the electric field ($E = V/L$) to reach the OP emission threshold energy ($\hbar\omega_{OP} \approx 0.18$ eV) [7], and the second term represents the temperature dependence of the spontaneous OP emission length. The OP emission MFP after an absorption event is obtained from Eq. 6 by replacing the first term with the OP absorption length of Eq. 4:

$$\lambda_{OP,ems}^{abs}(T) = \lambda_{OP,abs}(T) + \frac{N_{OP}(300)+1}{N_{OP}(T)+1}\lambda_{OP,300} \quad (7)$$

This approach lets us express the temperature dependence of the relevant MFPs with respect to the acoustic and optical scattering lengths at 300 K [7].

Fig. 2 illustrates the *I-V* characteristics of a typical (2 and 15 μm) long metallic tube. From this figure we observe that the current will be high in case of low length and fixed temperature at the constant background value (T_O).

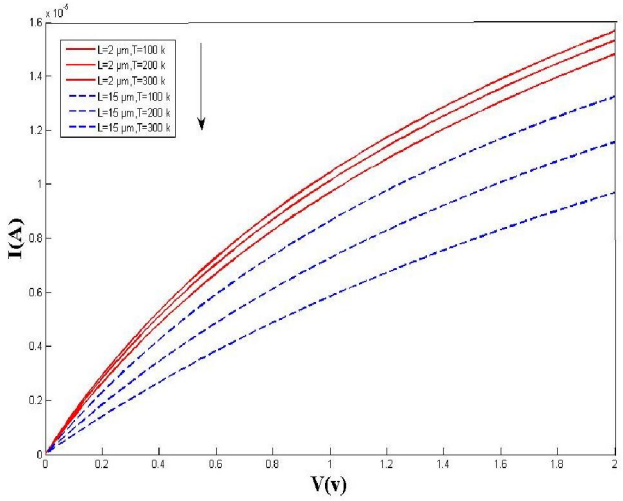

Fig. 2: Current-voltage model of a metallic SWCNT with L = 2, 15 μm and d = 2.4 nm in ambient T_O = 100, 200 and 300 K

Thermal Transport

The temperature profile along the SWCNT depends on the power dissipated, and hence on its resistance. We obtain this temperature profile by solving the heat conduction equation along the length of the tube, including heat generation from Joule self-heating and heat loss to the substrate. The expression of the steady-state Joule-heating equation with a temperature-dependent thermal conductivity along the length of the SWCNT is [9].

$$A\nabla(k_{th}\nabla T + p' - g(T - T_O)) = 0 \qquad (8)$$

where $A = \pi db$ is the cross-sectional area; d and b are the diameter and the tube wall thickness of the SWCNT, respectively. b≈0.34 nm, k_{th} is the SWCNT thermal conductivity where g is the net heat loss rate to the substrate per unit length.

The thermal conductivity of the SWCNT is expected to follow $k_{th} \approx 3600(300/T)$ $Wm^{-1}K^{-1}$ above room temperature.

We use $g \approx 0.15$ $WK^{-1}m^{-1}$ per tube length in our estimates for the small range of SWCNT diameters examined here. The Joule heating rate per unit length is $P' = I^2(R-R_C)/L$.

An analytic expression for the temperature profile $T(x)$ along the SWCNT can first be obtained if we make the simplifying assumption of uniform heat generation along the tube, using the boundary condition $T(-L/2) = T(L/2) = T_0$, the solution to (Eq. 8) can be written as[9]

$$T_{(X)} = T_o + \frac{p}{g}\left[1 - \frac{cosh(x/L_H)}{cosh(L/2L_H)}\right] \qquad (9)$$

For $-L/2 < x < L/2$, where T_0 is the temperature of the contacts at the two ends and $L_H = (k_{th}A/g)^{1/2}$ is the characteristic thermal healing length along the SWCNT

Eqs. (1) And (8) are solved along the length of the tube, and this iterative solution is repeated until the temperature converges within 0.1 K at each bias point. The current is then simply

$$I = (V/R) \qquad (10)$$

where I and R both depend on temperature (Fig. 3).

Novel Electro-Thermal Transport Model

The thermo-electric current (I_{hc}) caused by the temperature difference along the SWCNT interconnect will be taken into consideration in this work. The thermoelectric current (I_{hc}) equation is [10].

$$I_{hc} = NG_T\Delta T \qquad (11)$$

where N is the total number of acoustic modes (N = 4) [11] , ΔT is the temperature difference along the nanotube, and the thermal conductance quantum (G_T) is

$$G_T = \frac{\pi^2}{3}\frac{k_B^2 T}{h} \qquad (12)$$

It was found that the number of acoustic modes for all the tube structures having radius greater than 0.5 nm are four acoustic modes, while for nanotubes with lower radius only three acoustic modes are observed [11].

So, the new equation of the current will be $\boldsymbol{I = (V/R) + I_{hc}}$ (13)

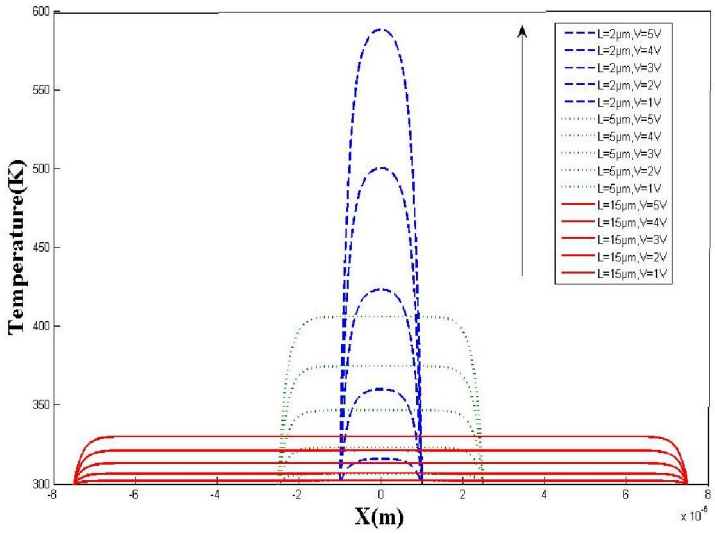

Fig. 3: Estimated temperature profiles along the SWCNTs when self-heating are included.
The profiles are computed at $V = 1, 2, 3, 4$ and 5 V from bottom to top (Eq. 8). The thermal healing length along the tube is $L_H \approx 0.2\ \mu m$ [7].

The flow chart shown in Fig. 4 illustrates the procedure of Novel electro-thermal transport model as follows: First, initial guess was assumed $\boldsymbol{T_{old}}$. Second, Calculate the temperature dependence of the resistance is obtained through the temperature dependence of the electron scattering Mean Free Paths (MFPs) with acoustic (AC) and optical (OP) phonons (Eq. 1). Third, Calculate the thermoelectric current ($\boldsymbol{I_{hc}}$) caused by the temperature difference along the SWCNT interconnect (Eq. 13). Fourth, Calculate the Joule heating rate per unit length. Fifth, calculate the thermal conductivity of the SWCNT above room temperature. Sixth, Calculate the temperature profile $\boldsymbol{T(x)}$ along the SWCNT is obtained if we make the simplifying assumption of uniform heat generation along the tube, using the boundary condition $\boldsymbol{T(-L/2) = T(L/2) = T_0}$ (Eq. 9). Finally, the new temperature was compared with the old one. If it converges, then Plot the temperature profile $\boldsymbol{T(x)}$ along the SWCNT. Otherwise, returned to second step

The temperature profile along the length of a SWCNT has been plotted when both ends are at the same temperature of 300 K.

The thermo-electric current ($\boldsymbol{I_{hc}}$) caused by the temperature difference along the SWCNTs interconnects (thermo-electric properties) is very important especially at low length ($\boldsymbol{L \leq 2\mu m}$) and high bias ($\boldsymbol{V \geq 3}$V). And it can be neglected at high length ($\boldsymbol{L \geq 15\mu m}$) and at any applied bias.

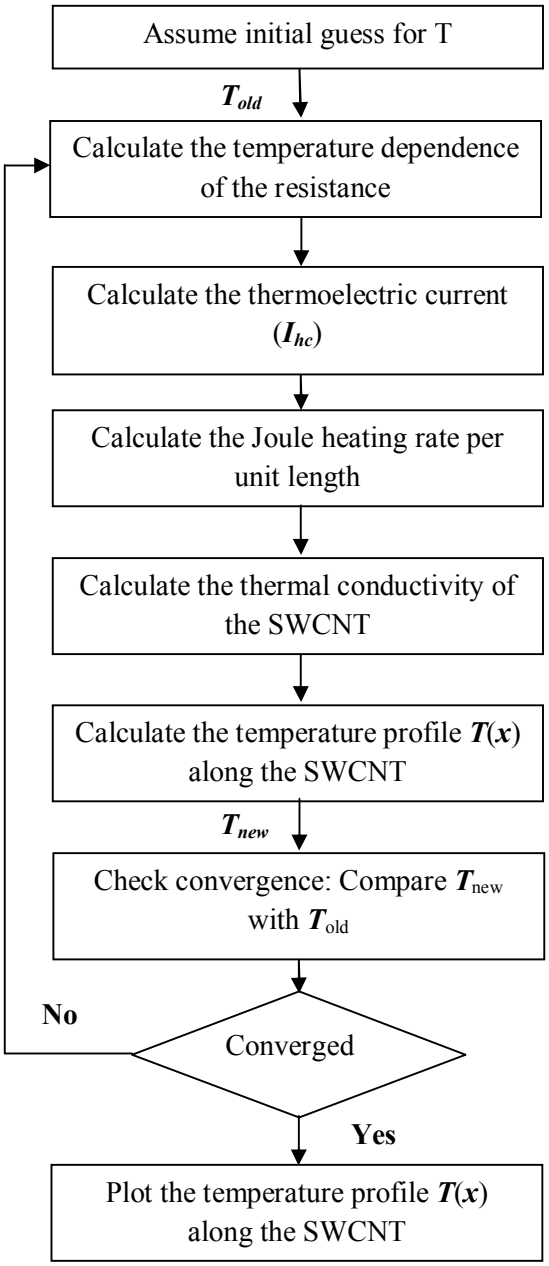

Fig. 4: Flow chart of Novel electro-thermal transport model

Results and Discussion

Eq. 13 will replace Eq. 10 in solving the system of equations, comparing the result of solving (Eqs. 1, 8 and 13) in this work with the solution of previous work (Eqs. 1, 8 and 10) at different lengths, this leads to change in the temperature distribution and the maximum temperature along the length of the tube. This change is shown at different lengths in Fig. (5.a, b and .c).

From these results we can observe that the thermo-electric current cannot be neglected at low length ($L \leq 2\ \mu m$) and high bias ($V \geq 3$V) as shown in Fig. 6. However, it can be neglected at high length ($L \geq 15 \mu m$) and at any applied bias as shown in Fig. 7.

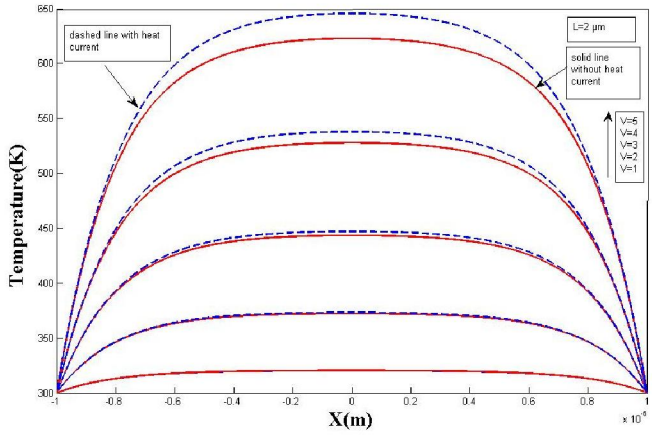

a

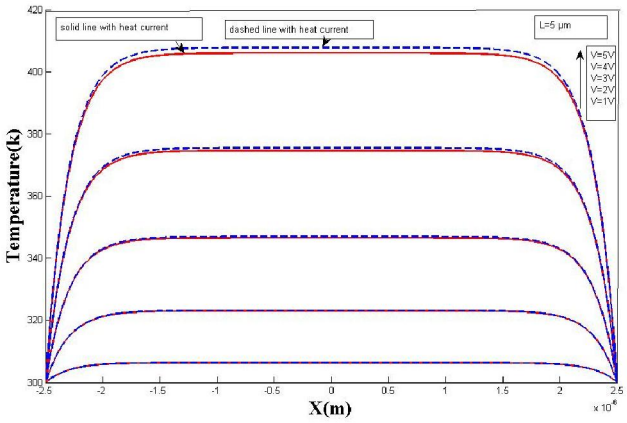

b

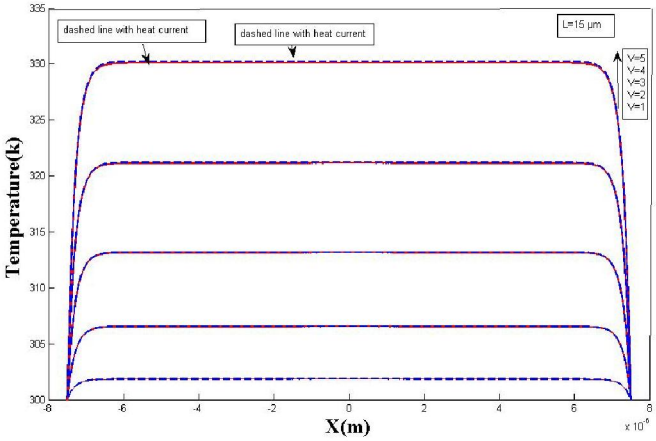

c

Fig. 5: Estimated temperature profiles along the SWCNTs at length of a) 2 μm, b) 5 μm and c) 15 μm

The maximum and average percentage difference (change) in temperature distribution between the result with the effect of thermo-electric current in this work and previous work without this effect at different lengths are shown in Tables 1, 2 and 3.

Table 1 at length L = 2 μm

V(V)	1	2	3	4	5
Max. Error (%)	0.0285	0.169534	0.718646	1.459319	2.437552
Avg. Error (%)	0.020281	0.237416	0.517542	1.060923	1.783326

Table 2 at length L = 5 μm

V(V)	1	2	3	4	5
Max. Error (%)	0.004921	0.038292	0.116276	0.242504	0.414727
Avg. Error (%)	0.004287	0.03339	0.101548	0.212217	0.363704

Table 3 at length L = 15 μm

V(V)	1	2	3	4	5
Max. Error (%)	0.000532	0.003833	0.011589	0.024695	0.043432
Avg. Error (%)	0.000506	0.003644	0.01102	0.023486	0.041315

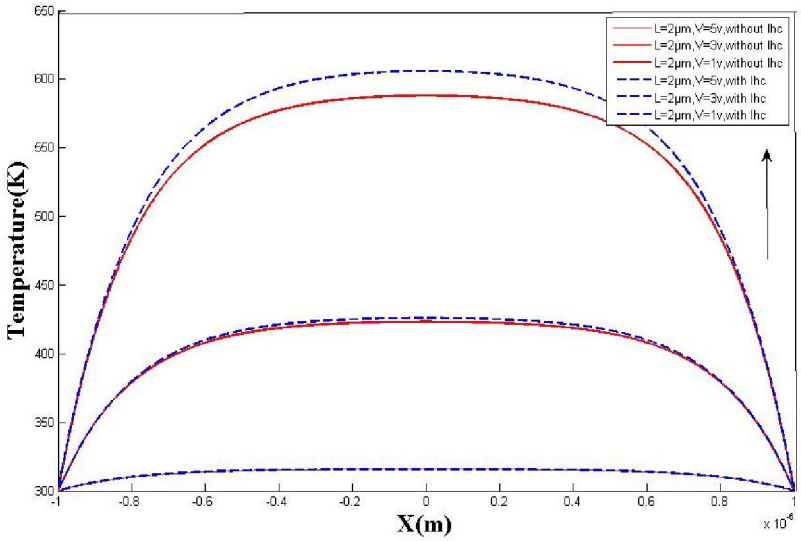

Fig. 6: Estimated temperature profiles along the SWCNTs at high length.

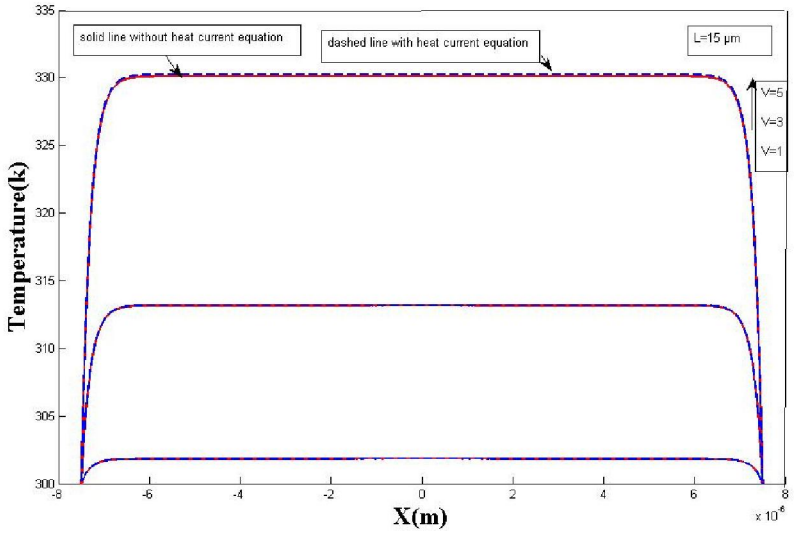

Fig. 7: Estimated temperature profiles along the SWCNTs at high length.

From these tables we can observe that the thermo-electric current cannot be neglected at small length ($L \leq 2\mu m$) and high bias ($V \geq 4V$). In contrary it can be neglected at high length ($L \geq 15\mu m$) and at any applied bias.

From studying the effect of changing T_O, we observed that decreasing T_O leads to decreasing the maximum temperature along the SWCNT while increasing T_O leads to increasing the maximum temperature along the SWCNT as shown in Fig. 8.

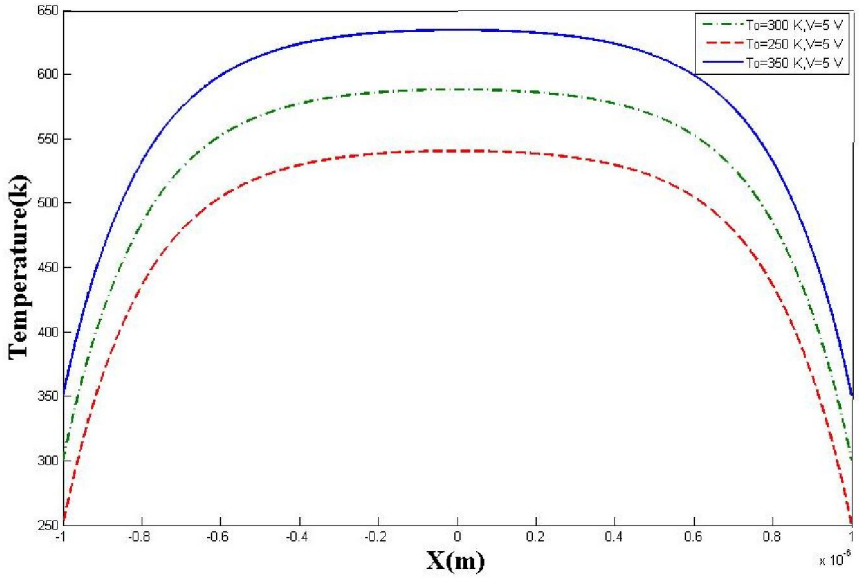

Fig. 8: Estimated temperature profiles along the SWCNTs at different T_O.

Conclusion

In this paper, a novel electro-thermal transport model in metallic SWCNTs which is relevant for practical interconnect applications ($1 < L < 15\mu m$) is presented. We observed that the current will be high in case of low length and fixed temperature at the constant background value (T_O), while self-heating at high bias must be taken into account for nanotube interconnects. In addition, the effect of thermo-electric current as a result of thermoelectric properties in this work shouldn't be neglected specially in case of small lengths ($\leq 2\ \mu m$) and high bias ($V \geq 3V$) while this effect can be neglected in high length ($\geq 15\ \mu m$) regardless of the bias.

Corresponding author
Walid Soliman
Engineering Physics and Mathematics Department, Faculty of Engineering, Ain Shams University, Cairo, Egypt.
walidsol@yahoo.com

References

1. Rekha Verma, Sitangshu Bhattacharya, and Santanu Mahapatra, IEEE, transactions on electron devices, vol. 59, no. 9, 2012.
2. Serhan Yamacli, Mutlu Avci, Physics Letters A 374, 297–304, 2009.
3. The international technology roadmap for semiconductors (ITRS) (Interconnect), *www.itrs.com*, 2011.
4. Hong Li, Wen-Yan Yin, Kaustav Banerjee, Jun-Fa Mao, IEEE Transactions on electron devices, vol. 55, no. 6, 2008.
5. Qing Cao, John A. Rogers, WILEY-InterScience, Advanced Materials, 21, 29–53, 2009.
6. F. Kreupl, A.P. Graham, G.S. Duesberg, W. Steinhögl, M. Liebau, E. Unger, W. Hönlein, Elsevier Science, Microelectronic Engineering 64, 399–408, 2002.
7. Eric Pop, David Mann, John Reifenberg, Kenneth Goodson and Hongjie Dai, IEDM, 2005.
8. Eric Pop, David Mann, jien Cao,Qian Wang, Kenneth Goodson, and Hongjie Dai, IEDM, PRL 95, 155505, 2005.
9. Rekha Verma, Sitangshu Bhattacharya, and Santanu Mahapatra, IEEE, Transactions on electron devices, vol. 58, no. 11, 2011.
10. Prabhakar R. Bandaru, American Scientific Publishers, Journal of Nanoscience and Nanotechnology, vol.7, 1–29, 2007.
11. Prapti Saxena and Sankar P Sanyal, Indian Academy of Sciences, Pramana, Journal of Physics, vol. 67, no. 2, pp. 305-317, 2006.

2/15/2013